ACS APPLIED MATERIALS & INTERFACES

Research Article

www.acsami.org

Optimization of PEDOT Films in Ionic Liquid Supercapacitors: Demonstration As a Power Source for Polymer Electrochromic Devices

Anna M. Österholm,* D. Eric Shen, Aubrey L. Dyer, and John R. Reynolds

School of Chemistry and Biochemistry, School of Materials Science and Engineering, Center for Organic Photonics and Electronics, Georgia Institute of Technology, Atlanta, Georgia, 30332 United States

Supporting Information

ABSTRACT: We report on the optimization of the capacitive behavior of poly(3,4-ethylenedioxythiophene) (PEDOT) films as polymeric electrodes in flexible, Type I electrochemical supercapacitors (ESCs) utilizing ionic liquid (IL) and organic gel electrolytes. The device performance was assessed based on figures of merit that are critical to evaluating the practical utility of electroactive polymer ESCs. PEDOT/IL devices were found to be highly stable over hundreds of thousands of cycles and could be reversibly charged/discharged at scan rates between 500 mV/s and 2 V/s depending on the polymer loading. Furthermore, these devices exhibit leakage currents and self-discharge rates that are comparable to state of the art electrochemical double-layer ESCs. Using an IL as device electrolyte allowed an extension of the voltage window of Type I ESCs by 60%, resulting in a 2.5-fold increase in the energy density obtained. The efficacies of tjese PEDOT ESCs were assessed by using them as a power source for a high-contrast and fast-switching electrochromic device, demonstrating their applicability in small organic electronic-based devices.

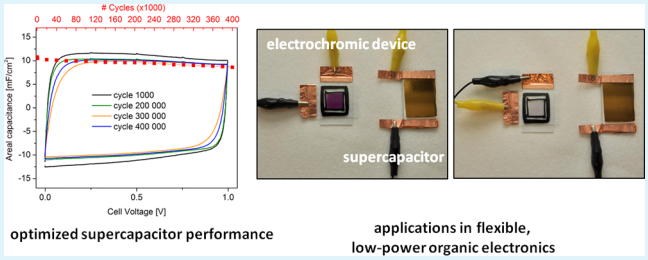

KEYWORDS: *dioxythiophenes, electrochemical supercapacitors, ionic liquids, electrochromic devices, charge storage, organic electronics*

INTRODUCTION

Electroactive conjugated polymers (EAPs) have shown great promise as active materials in flexible, lightweight, and easily processed devices for applications ranging from organic photovoltaics,[1,2] to electrochromics,[3,4] and charge storage,[5−7] to name a few. Electrochemical supercapacitors (ESC) are charge storage devices that bridge the gap between conventional batteries (high energy density, low power density) and capacitors (high power density, low energy density).[6−8] ESCs typically have lower energy densities than batteries but they can be rapidly charged/discharged and have significantly longer cycle lives. There are two types of ESCs: (i) electrochemical double-layer capacitors that store charge in the electrochemical double layer between a porous electrode (typically a high surface area carbon) and the electrolyte,[9] and (ii) electrochemical redox supercapacitors that store charge using materials such as transition metal oxides (e.g., RuO_x and MnO_2) or EAPs.[6−8] As the charge accumulation is purely electrostatic in double-layer ESCs, the amount of charge stored, and consequently, the energy density of the device is limited by the available surface area of the electrode material. For this reason, there has been a growing interest in using pseudocapacitive materials with higher capacitance. Other desired properties are fast charge/discharge rates (t < 60 s), high cycle life (>10^5 cycles), lightweight, high reliability, and low cost.[10]

EAPs are attractive candidates for ESCs, not only because they exhibit pseudocapacitance but also for their fast switching between redox states, moderately high conductivities in the charged state, and the possibility for inexpensive and easy manufacturing. In addition to EAPs, inorganic transition-metal oxides have also shown promise as alternative pseudocapacitive electrode materials in ESCs. In contrast to EAPs, metal oxides store charge on the oxide surface and not in the bulk of the electrode material. Consequently, fabrication is limited to using either very thin metal oxide films or nanostructuring the films to create higher surface areas.[11] Furthermore, transition-metal oxides typically suffer from poor electrical conductivity, which limits the charge/discharge rates needed for high power applications. EAPs as active materials in ESCs were first studied by Ferraris, Gottesfeld, and co-workers,[5,12] and ever since there has been a continuous and increasing interest in using EAPs for charge storage. The redox process (doping/dedoping) occurring during charging/discharging of an EAP is a combination of charge injection into the polymer backbone from the current collector and ion exchange from the electrolyte to maintain charge neutrality in the EAP film. The nature of this redox reaction requires that the EAP has high

Received: October 3, 2013
Accepted: December 5, 2013
Published: December 12, 2013

electronic and ionic conductivities to be able to maintain fast charge/discharge rates, a crucial property for ESCs. The charge/discharge rates are governed by mass transport of ions through the EAP film, and consequently, the rate is highly dependent on film morphology[13,14] and type of electrolyte.

Commercially available ESCs have discharge times that are <30 s; hence, the discharge time of a pseudocapacitive ESC should be in the same range to adequately evaluate feasibility of the device.[15] In addition to the electrolyte being important for charge/discharge rates (i.e., power density, $P = E/t_{discharge}$, where E is energy density), it also determines the operating voltage. Given that energy density is quadratically proportional to the voltage ($E = 1/2CV^2$), organic electrolytes are more widely used than aqueous ones, as the former can sustain higher voltages. Propylene carbonate (PC) and acetonitrile (ACN) with dissolved quaternary alkyl ammonium salts are typically used in commercial ESCs, but voltages higher than 3 V have not been realized with these conventional electrolytes.[16] More recently, ionic liquids (ILs) have been evaluated for ESCs, as they offer the promise of improved safety over organic electrolytes because of their low vapor pressure and low flammability. Additionally, ILs possess moderate intrinsic conductivity and many are redox-robust and stable over a broad temperature range.[16−18] Finally, ILs are promising electrolytes in EAP-based electrochemical devices, as several EAPs have shown improved cycling stability in ILs compared to organic electrolytes.[17,19−22]

Since the conversion between the doped and undoped states in an EAP is governed by the transport of counterions through the film, a three-dimensional morphology is expected to increase the charge/discharge rates and ultimately the power density. One simple method of obtaining a 3D-morphology is through electrochemical polymerization. This method enables deposition of thick, well-adhering films on a number of different electrode substrates. In addition, it is an accurate and precise deposition method that requires small amounts of starting material. The electrochemistry and electrochemical polymerization of one polymer in particular, poly(3,4-ethylenedioxythiophene) (PEDOT), has been thoroughly reviewed.[23] Although PEDOT and its derivatives tend to exhibit lower specific mass capacitance than, for example, poly(aniline) (PANI),[7] the literature on PEDOT as a charge storage material has grown rapidly over recent years. PEDOT is electroactive with a high capacitance over a broad voltage range, it exhibits high chemical and thermal stability, and it is compatible with both aqueous and organic electrolytes.[23] Because of its high stability in the oxidized state, PEDOT is a promising electrode material for symmetric Type I and asymmetric Type II ESCs;[6,12] it has also been tested in hybrid devices with activated carbon as the counter electrode.[24] Since the first electrochemical polymerization of EDOT was reported in 1991,[25] a large family of poly(3,4-alkylenedioxythiophenes) (PXDOTs), structurally similar to PEDOT, has been synthesized, and several PXDOTs have been evaluated as charge storage materials in ESCs. PEDOT and PXDOT based devices exhibit fast charge/discharge rates (<2 s) and lifetimes exceeding 50 000 cycles.[20,26] It has been demonstrated that some of the shortcomings of conjugated polymer ESCs (for example a limited voltage range) can be addressed by constructing tandem modules where ESCs in series or parallel enables the extension of the cell voltage and the device currents, respectively, by a factor of 4.[26] Finally, it has been shown that PXDOT ESCs can be operational between −35 and +60 °C by using ILs as the device electrolyte.[27]

Here, we report on the optimization of a Type I PEDOT-based ESC in a flexible device architecture using IL or organic gel electrolytes. Depending on the amount of PEDOT deposited on the respective electrodes, we are able to fabricate devices that charge/discharge in 0.5−2 s. Increasing the thickness of the PEDOT layer increases the overall charge that can be stored but it also slows down the rate at which the device can be reversibly charged/discharged. Use of an IL electrolyte increased the cell voltage of a Type I ESC from 1.0 to 1.6 V. In addition, our PEDOT ESCs have self-discharge rates and leakage currents comparable to commercially available double-layer ESCs as well as superior cycling stability of 400 000 cycles. Finally, the efficacies of our PEDOT ESCs are assessed by using them as a power source for EAP-based electrochromic devices, demonstrating their applicability in small organic electronic-based devices.

EXPERIMENTAL SECTION

Materials. 3,4-Ethylenedioxythiophene (98%), purchased from AK Scientific, was distilled under vacuum prior to use. Lithium bis-(trifluoromethylsulfonyl)imide (LiBTI) was purchased from Acros Organics and used as received. Tetrabutylammonium hexafluorophosphate (98%, Alfa Aesar) was purified by recrystallization from hot ethanol. Propylene carbonate (PC) and acetonitrile (ACN) were purchased from Acros Organics and Fisher Scientific and purified using a solvent purification system from Vacuum Atmospheres. Poly(methyl methacrylate) (PMMA, M_w: 996,000), used in the fabrication of the gel electrolyte, was purchased from Sigma Aldrich. Gold coated Kapton (Au 1000 Å; 1 mil Kapton/3M 966 adhesive) substrates were purchased from Astral Technology Unlimited. Electrode contacts were made using conductive copper tape (3M).

Electrode Fabrication and Device Assembly. All electrochemistry was performed using a PAR 273A potentiostat/galvanostat. The electropolymerization of EDOT was performed in a three-electrode cell using a Pt mesh counter electrode and a Ag/Ag^+ reference electrode (containing 10 mM $AgNO_3$ in 0.5 M LiBTI/ACN) that was calibrated versus ferrocene ($E_{1/2}$: +85 mV). For the film optimization, a glassy carbon (GC) or Au button electrode, polished to a mirror finish, was used as the working electrode. For the device optimization, PEDOT was electrodeposited on Au/Kapton with a predefined surface area of 2.83 cm^2. Cu tape was used as contact material. The extent of the PEDOT electropolymerization was controlled by monitoring the charge consumed during the polymerization. The film thickness and surface roughness were determined by stylus profilometry (Bruker DektakXT). A few drops of electrolyte (0.5 M LiBTI/PC, 0.5 M LiBTI/PC/6% PMMA, or neat 1-ethyl-3-methyl-imidazolium bis-(trifluoromethylsulfonylimide) ([EMI][BTI])) were placed on each of the electrodes that were then sandwiched together and separated using a polypropylene separator (5 μm AN50 from Millipore). For the gel electrolyte devices, the PEDOT films were deposited from 0.5 M LiBTI/PC and for the IL devices from 0.5 M [EMI][BTI]/PC. All devices were fabricated and tested in air.

[EMI][BTI] Synthesis. The synthesis of [EMI][BTI] was based on a literature procedure.[28] 1-Ethyl-3-methyl-imidazolium chloride (EMICl) (20.00 g), purchased from Sigma-Aldrich (98%), was dissolved in approximately 100 mL of deionized water in a 250 mL round-bottom flask. To this solution, 5.0 g of decolorizing charcoal was added. The solution was then heated to reflux while mixing for 12 h. After cooling, the solution was vacuum filtered through a pad of Celite 545 to remove the charcoal. This step was repeated as necessary to remove residual yellow color. LiBTI (47.15 g), from Acros Organics (99%), was added to the EMICl followed by 50 mL of deionized water. This solution was then stirred at ambient temperature for 3 h. After mixing had ceased, two layers had formed. These layers were

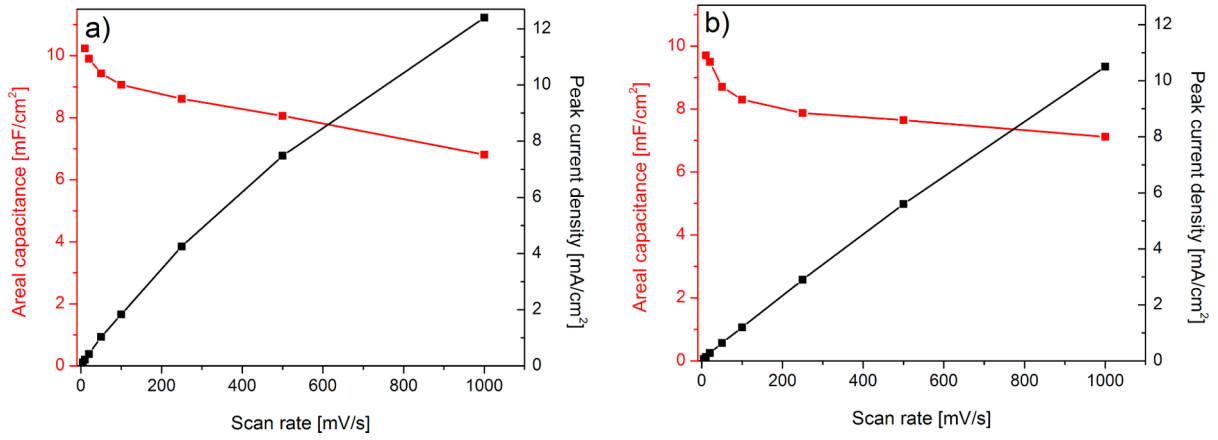

Figure 1. Effect of increasing scan rate on the peak current density and areal capacitance for PEDOT films deposited and cycled in (a) 0.5 M LiBTI/PC and (b) 0.5 M [EMI][BTI]/PC.

transferred to a separatory funnel and dichloromethane (DCM) was added. The lower layer was extracted three times and then passed through silica (Sorbent Technologies). The DCM was removed under vacuum and the remaining liquid was heated under vacuum at 60 °C overnight. The purity of the IL was verified using fluorescence spectroscopy, UV−vis spectroscopy, and electrochemistry. The potential window for the [EMI][BTI] was determined by cyclic voltammetry to be 4.3 V, which is in good agreement with potential stability values reported for this IL.[16,18,29,30]

Electrochromic Device Fabrication. Electrochromic devices (ECDs) were fabricated by adapting an architecture previously reported in the literature, wherein an electrochromic ProDOT-based polymer (ECP-Magenta)[31] served as the working electrode, while a pyrrole-based minimally color-changing polymer (MCCP)[32] served as a charge-balancing counter electrode. Two ITO/glass slides (25 × 75 × 0.7 mm, Rs = 8−12 Ω/sq) from Delta Technologies were cleaned by rinsing first with toluene, followed by acetone and finally isopropanol. Polymer solutions were prepared from 5 mg/mL of polymer in toluene, which was left to stir for three hours without heating, before passing through a 0.45 μm PTFE filter. An area of 1.61 cm^2 was masked off with tape and the ECP-Magenta and the MCCP solutions were sprayed with an airbrush to 250 nm thicknesses. The tape was removed and the films transferred to a glovebox. A polyisobutylene ADCO sealant was applied along the edges of one of the ITO/glass slides to serve both as a barrier to oxygen and moisture, and as a separator between the two electrodes.[33] Gel electrolyte (0.5 M LiBTI in PC and 6% PMMA) was added and the two ITO/glass slides were pressed together and heated on a hot plate at 100 °C for no more than 10 min to activate the sealant. The device was removed from the glovebox and copper tape applied to the ITO/glass to serve as contacts.

RESULTS AND DISCUSSION

Polymer Electrode Optimization. For the PEDOT optimization, the deposition variables that were explored included monomer concentration (10 or 50 mM), electrolyte (type and concentration), solvent, deposition method, and deposition charge. The electrolytes evaluated were $TBAPF_6$ and LiBTI dissolved in either ACN or PC at a concentration of 0.1 or 0.5 M. EDOT was electropolymerized by cyclic voltammetry (−1.2 V to +1.2 V at 50 mV/s), galvanostatic polymerization (0.2−1 mA/cm^2), or potentiostatic polymerization, with the optimal potential for the potentiostatic polymerization determined by evaluating a series of potentials ranging from 0.85 to 1.0 V. The amount of deposited polymer was controlled by monitoring the charge passed during the polymerizations. The charge densities evaluated were 120, 360, 480, 650, and 960 mC/cm^2. After electropolymerization, the films were rinsed with ACN or PC and the redox behavior was evaluated by cyclic voltammetry in monomer-free electrolyte solution to determine the film capacitance, scan rate dependence behavior, reproducibility, and repeatability. All experiments were performed in triplicate to verify the repeatability of the polymerizations. Through this analytical, quantitative, and statistically accurate approach, we were able to determine the best deposition parameters for the PEDOT films that were to be used in the device optimization. We found that the most reproducibly prepared, well-adhered, and electroactive materials were generated using 50 mM EDOT dissolved in 0.5 M LiBTI-PC deposited via potentiostatic polymerization at 0.9 V vs Ag/Ag^+. The type of electrolyte had a negligible effect on the film capacitance, but it had a significant effect on the film adhesion on both GC and Au electrodes. Polymerizing to charge densities higher than 360 mC/cm^2 in the presence of $TBAPF_6$ resulted in PEDOT films that delaminated from the electrode upon drying. A good film adhesion is crucial for being able to reproducibly deposit thick and highly electroactive PEDOT films.

The electrolyte is a key component in any electrochemical device because it determines the available voltage and temperature range, charge/discharge rates, and stability of the device. [EMI][BTI] is regarded as a promising electrolyte candidate for EAP-based ESC devices exhibiting superior cycling stability over a broad temperature range.[18,20] For this reason, we chose to evaluate [EMI][BTI] as an alternative to LiBTI/PC. We compared PEDOT films deposited from 0.5 M LiBTI/PC to PEDOT films deposited from 0.5 M [EMI]-[BTI]/PC. Supporting Information Figure S1 shows the cyclic voltammograms (CVs) of these films deposited using a charge density of 120 mC/cm^2 in the two electrolyte systems. The areal capacitance was obtained by dividing the total amount of charge passed during film charging by the potential window. Both electrolyte systems give PEDOT films with approximately the same areal capacitance, 10 $mF/cm^2 \pm 1$ mF/cm^2 at 50 mV/s. Figure 1 shows the scan rate dependence (10−1000 mV/s) of the peak current density and the areal capacitance of PEDOT deposited and cycled in LiBTI/PC (Figure 1a) and in [EMI][BTI]/PC (Figure 1b). The corresponding CVs can be found in Supporting Information Figure S2. In Figure 1a, when LiBTI/PC is used as the electrolyte, a linear relationship between peak current and scan rate is observed up until scan

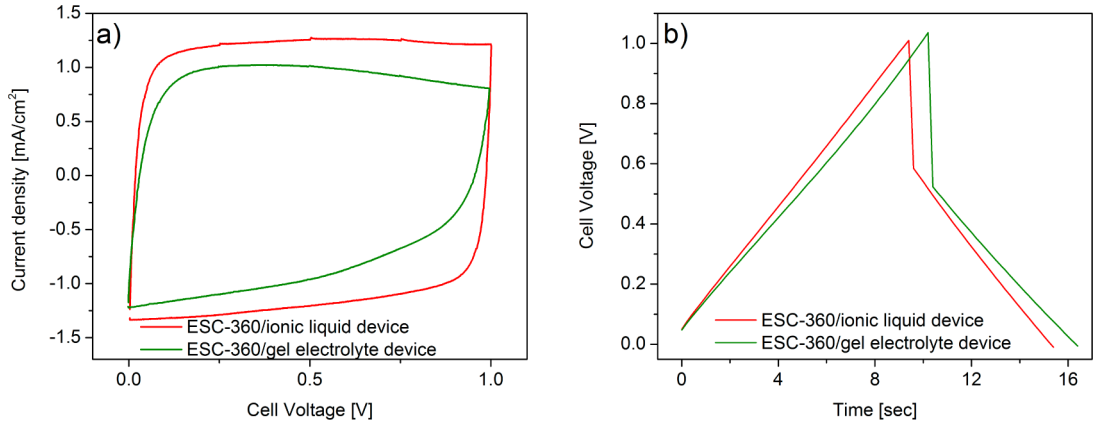

Figure 2. (a) Comparison of Type I PEDOT ESCs with different electrolytes. Representative CVs of device charging at 100 mV/s in a 1.0 V window. (b) Galvanic charging/discharging curves for two PEDOT ESCs to 1.0 V at 1 mA/cm^2.

rates of 250 mV/s after which the behavior is found to deviate from linearity. In Figure 1b, on the other hand, a linear dependence between the peak current and the scan rate is observed even at scan rates as high as 1 V/s indicating that the redox process is surface-controlled (i.e., nondiffusion limited). From the areal capacitance versus scan rate plot, the PEDOT film cycled in [EMI][BTI]/PC is able to retain more of its initial capacitance as the scan rate is increased. The surface roughness and film thicknesses were probed by stylus profilometry (see Supporting Information Figure S3) to evaluate if changing the deposition electrolyte from LiBTI to [EMI][BTI] would noticeably affect either of these properties. The film thickness and surface roughness are both approximately 40% higher for PEDOT deposited in [EMI][BTI]/PC. Given that the amount of deposited PEDOT is the same, but the film deposited in [EMI][BTI] is thicker, it suggests that a more porous PEDOT film is formed in [EMI][BTI]/PC. This could account for the slight improvement in the capacitance retention observed at higher scan rates. Seeing that the difference in the electrochemistry of PEDOT in the two electrolyte systems is small, we proceeded to optimize two sets of devices, one using LiBTI/PC or LiBTI/PC/PMMA gel electrolyte and one set using neat [EMI][BTI] as device electrolyte.

Device Comparison. Reporting the mass capacitance, energy density, and power density per weight of just the EAP fails to give a realistic picture of device performance, especially since the mass of electrochemically polymerized films is in the μg−mg range. Also, given that (i) EAP-based ESCs are interesting for flexible and lightweight energy storage and (ii) the area of the electrode that is coated by an EAP can be consistently reproduced, it is more relevant to report areal capacitance than the specific mass capacitance for our devices. For an ideal ESC, the current should be independent of the voltage; that is, the charging/discharging CV should be rectangular and the galvanic charge/discharge curves should be symmetrical. Curvature at the corners of the CV is a sign of an internal resistance in the device (equivalent series resistance, ESR). In a galvanic charge/discharge plot, the ESR is observed as a voltage drop at the beginning of the discharge curve. EAP-based ESCs rarely exhibit perfectly rectangular CVs because of the nature of the pseudocapacitive redox reaction, electrolyte resistance, possible interfacial resistance between the current collector and the EAP film, ionic diffusion resistance in the EAP film, and ionic resistance of ions moving through the separator.

A charging/discharging CV and a galvanic charge/discharge curve for two Type I ESCs with different device electrolytes are compared in Figure 2. The devices shown in Figure 2 have PEDOT films that have been deposited using a polymerization charge of 360 mC/cm^2; these devices are referred to as ESC-360. As the CVs are not perfectly rectangular, the areal capacitance was obtained by dividing the total amount of charge passed during charging by the potential window (1.0 V). ESC-360 devices (regardless of the electrolyte) have areal capacitances of 10.5 ± 1 mF/cm^2. As can be seen in Figure 2a, neither of the devices give rise to perfectly rectangular CVs; however, the CV of ESC-360 with neat [EMI][BTI] appears closer to ideality than the ESC-360 with the gel electrolyte. This deviation from ideal behavior can be attributed to an increased resistance in the device.

The rectangularity and resistance can be quantified by assessing the fill factor (FF) of the device CV. In the photovoltaics field, the FF is a key parameter in evaluating the performance of a solar cell and is defined as the ratio of the maximum obtainable power to the ideal maximum power. By analogy, the FF in ESCs can be defined as the ratio of the actual charge passed during device operation to the charge passed under ideal device behavior, as shown in Figure 3. Additionally, a FF can be separately defined for both the charging and the

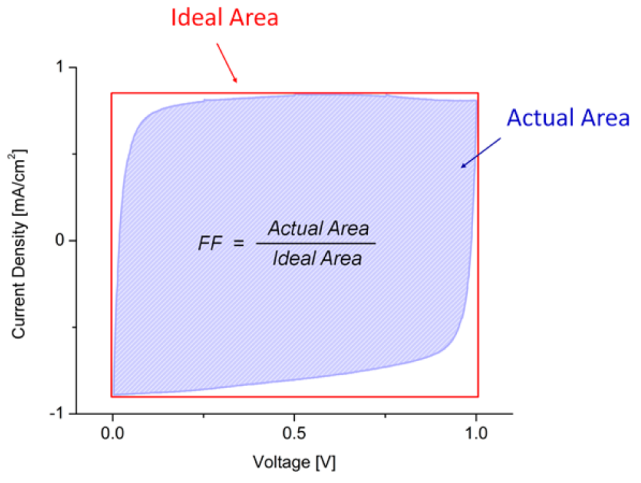

Figure 3. Estimating fill factor from a charge discharge CV as the ratio of the actual area within the CV curve (shaded in blue) to the ideal area defined by the rectangle (shown in red).

dx.doi.org/10.1021/am4043454 | ACS Appl. Mater. Interfaces 2013, 5, 13432−13440

discharging processes. We propose that estimating and using the FF of an ESC CV will be an effective way of evaluating, quantifying, and comparing device performances across the field. The FFs estimated from the CVs in Figure 2a were 86% for the ESC-360/IL device and 70% for the ESC-360/gel electrolyte device, demonstrating that using the IL as device electrolyte improved the FF 1.22 times and confirming that this device is less resistive. The galvanic charge/discharge curves recorded at a current density of 1 mA/cm^2 (Figure 2b) are in good agreement with the CVs; there is a large voltage drop upon discharging both devices suggesting a significant ESR. The ratio of the resistances is 1.19 and hence in excellent agreement with the ratio of the FF estimated from Figure 2a. This supports the usage of FF as a way to quantify ESR and deviation from ideality in ESCs.

As the viscosity of the gel electrolyte is an order of magnitude higher than that of the IL, we made devices using 0.5 M LiBTI/PC (without PMMA) as electrolyte to determine if the differences in FFs in Figure 2a are viscosity related. The liquid electrolyte devices have the same capacitances and charge/discharge rates as the devices with gel electrolyte. It has been shown that conductive gels containing lithium salts such as LiBTI exhibit high ionic conductivity comparable to liquid electrolytes using the same salt.[34] The ionic conductivities of [EMI][BTI] and 0.5 M LiBTI/PC are approximately 8.5 and 7 mS/cm, respectively.[16,30,34] Therefore, the differences in FF between the IL and the gel electrolyte device, and the asymmetry in the charging and discharging CV curves of the gel electrolyte devices, are attributable to more subtle factors such as the identity of the ions in the electrolyte and how these interact with the PEDOT films, rather than just the conductivity and viscosity of the electrolytes.

The ability of the PEDOT ESCs to maintain their areal capacitance even at rapid charging/discharging depends on the rate of mass transport through the film and hence on the film thickness. Figure 4 shows three PEDOT/IL devices made with

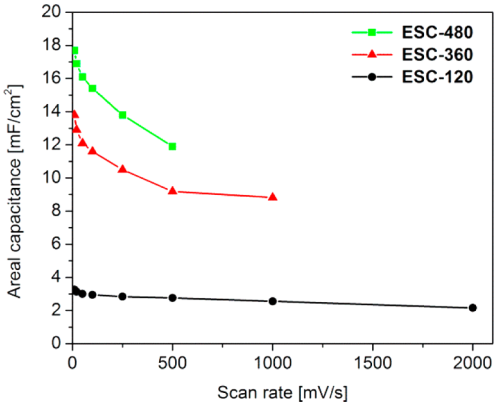

Figure 4. Effect of amount of PEDOT (polymerization charge density: 120, 360, or 480 mC/cm^2) on the areal capacitance of PEDOT/IL ESCs with increasing scan rate.

different amounts of PEDOT. A device made by depositing 120 mC/cm^2 of PEDOT on both current collectors (ESC-120) exhibits only a minimal decrease in areal capacitance as the scan rate is increased from 5 mV/s to 2 V/s, the latter being equal to a discharge time of 0.5 s. Slower scan rates than 20 mV/s result in charge/discharge times of nearly one minute and are not comparable to rates of a commercially available ESC. Hence, estimating the device capacitance from CVs recorded using scan rates slower than 20 mV/s is unrepresentative. An ESC-360 can be reversibly charged/discharged at 1 V/s but, at this scan rate, the device is only capable of maintaining 75% of its capacitance. Increasing the polymerization charge density to 480 mC/cm^2 (ESC-480), results in a device that cannot be reversibly charged/discharged at 1 V/s. The estimated energy and power density values for the three devices are listed in Table 1, assuming a device weight of 500 mg. As expected, the

Table 1. PEDOT Device Performance

device	energy density at 50 mV/s (Wh/kg)	energy density at max mV/s (Wh/kg)	power density at 50 mV/s (W/kg)	power density at max mV/s (W/kg)
ESC-120	0.24×10^{-2}	0.16×10^{-2}	0.43	12.23
ESC-360	0.95×10^{-2}	0.69×10^{-2}	1.71	24.96
ESC-480	1.27×10^{-2}	0.93×10^{-2}	2.28	16.84

energy density increases as we increase the amount of PEDOT loading, however, the power density at maximum scan rate does not. Rather, the highest power density was found for ESC-360. The trend is the same for the gel electrolyte devices.

As mentioned previously, the energy density is quadratically proportional to the voltage and, as such, efforts toward maximizing the cell voltage are of great importance. One approach for increasing the voltage window is to couple several Type I ESCs in series.[26] This allows for an extension of the voltage window, but the module displays a lower current density than a single device. It has been shown that EAP films can be reversibly cycled in a much broader potential window when using an IL instead of ACN or PC based electrolytes.[19] Figure 5 shows an ESC-360/IL device (Figure 5a) and an ESC-360/gel electrolyte device (Figure 5b) charged/discharged to cell voltages up to 1.6 V. The ESC-360 with [EMI][BTI] can be reversibly charged/discharged up to 1.6 V without compromising the device capacitance. While the FF decreases by 14%, the increased voltage window affords an improvement in the energy density by a factor of 2.5, as well as an improvement in the power density by a factor of 1.6. In contrast, the ESC-360/gel electrolyte begins losing device capacitance at voltage windows above 1.1 V.

When considering charge storage applications, rechargeable batteries have higher energy densities but low power densities as a result of their slow charge/discharge rates; additionally, they can only be used for 100−1000 cycles. In the EAP literature, a poor cycling stability is typically attributed to mechanical breakdown of EAP films as a result of the constant swelling/shrinking occurring as ions and solvent molecules are inserted/expelled during potential cycling.[7] However, several studies have shown that ESCs based on PXDOTs can be successfully charged/discharged over extended periods of time. Pandey and Rastogi[35] monitored the discharge capacity of a solid-state PEDOT ESC and found that after an initial decrease in capacitance during the first few cycles, a relatively stable capacitance was maintained over 10 000 cycles. Liu and Reynolds reported a Type I ESC with poly(2,2-dimethyl-3,4-propylene-dioxythiophene) (PProDOT-Me$_2$) as active material (electrolyte [EMI][BTI]/PC) that was able to retain 85% of its initial capacitance over 32 000 cycles at 78% depth of discharge.[26] Stenger-Smith et al.[20] reported a Type II PEDOT-PProDOT ESC where the charge capacity was

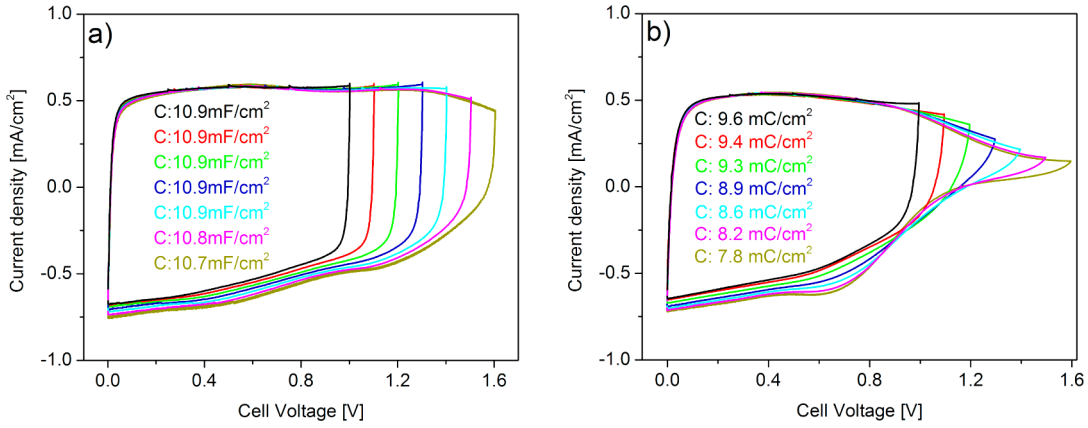

Figure 5. Effect of cell voltage (at 50 mV/s) on device capacitance for (a) ESC-360/IL and (b) ESC-360/gel electrolyte.

measured for 50 000 cycles between 0 and 0.5 V. With [EMI][BTI] as electrolyte, the ESC was able to retain 98% of its initial capacitance after 50 000 cycles. Interestingly, with a LiBTI-based gel electrolyte a similar device lost 30% of capacitance over the same number of cycles. In this study, the cycling stability of an ESC-360/IL (fabricated and tested in air) was monitored over 400 000 cycles between 0 and 1.0 V at 100 mV/s as shown in Figure 6. After an initial capacitance drop of 4.8% during the first 10 000 cycles, we only observed a 3−4% drop in capacitance for every 100 000 cycles. After 400 000 cycles, the device managed to retain 80% of the initial capacitance. The improved stability could in part be attributed to lower volume changes reported for EAPs when using solvent-free electrolytes.[19] Recently, Irvin and Carberry[36] showed that PEDOT cycled in neat [EMI][BTI] exhibited cation-dominated transport during oxidation instead of anion-dominated transport that is typically observed when using solution-based organic electrolytes. Previously, a cation-dominated transport has also been observed for EAP actuators and films in [EMI][BTI] along with lower degrees of swelling and shrinking during cycling.[37−39] Lower volume changes in the oxidized state should result in less mechanical stress, which may explain why our PEDOT-ESCs are stable over 400 000 cycles.

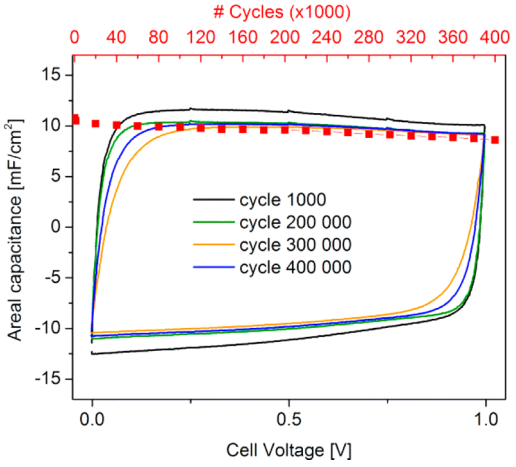

Figure 6. Cell lifetime of an ESC-360/IL monitored over 400 000 cycles between 0 and 1.0 V at 100 mV/s.

Other important parameters for the practical use of ESCs are the self-discharge rate and the leakage current. These figures-of-merit are often overlooked in EAP ESC research. In theory, ideal capacitors should maintain a constant voltage without any current flow from an external circuit. In practice, ESCs do require a small current, so-called leakage current, to be able to maintain a constant voltage. This leakage current will slowly cause a charged ESC to discharge if not connected to an external power source. The self-discharge (monitored for 24 h) and the leakage current (monitored for 12 h) for an ESC-360/IL are shown in Figure 7a and b, respectively. During the 24 h

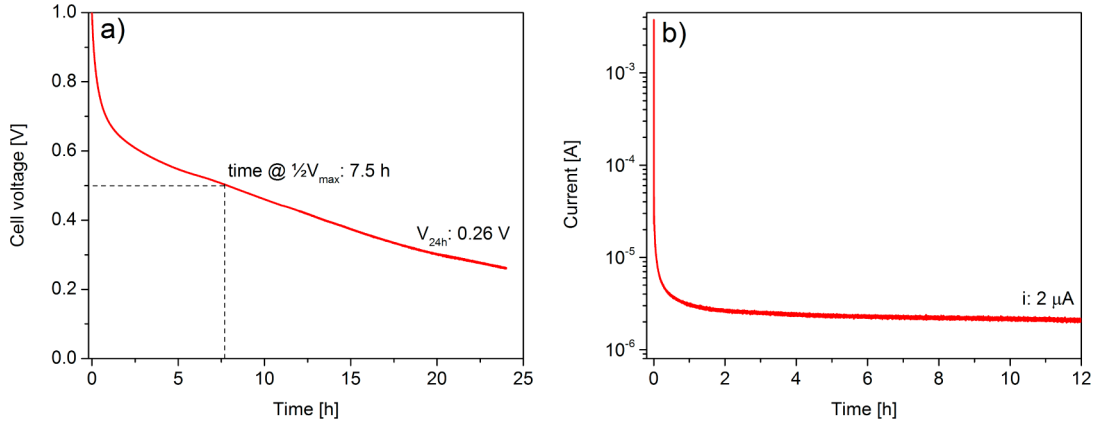

Figure 7. (a) 24 h self-discharge for ESC-360/IL charged to 1.0 V for 30 min. (b) Leakage current measurement of ESC-360/IL initially charged to 1.0 V for 12 h.

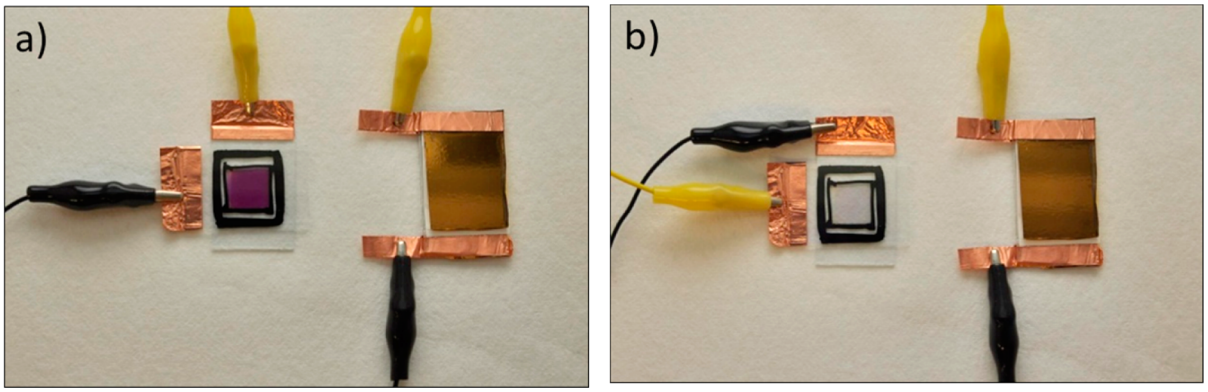

Figure 8. Photographs of the ESC-ECD assembly with the ECD (a) in its colored state and (b) in its colorless state.

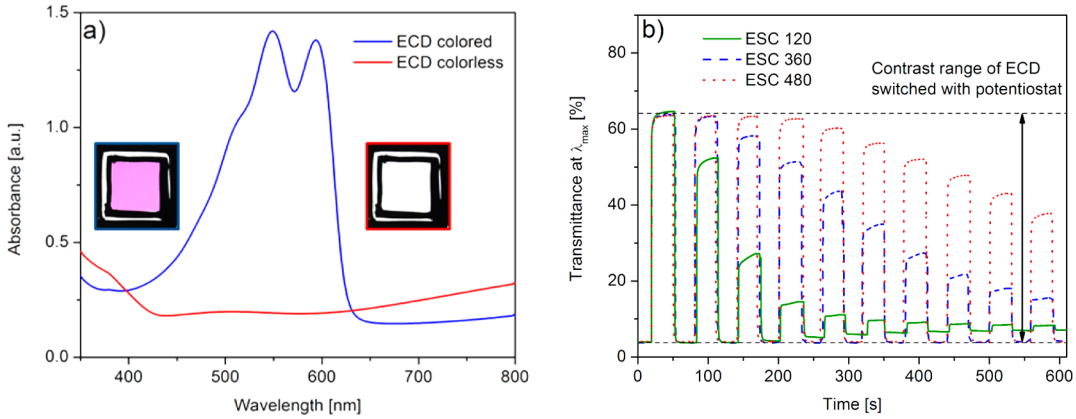

Figure 9. (a) Spectra and photographs of the ECD in its fully colored and fully colorless states switched using an ESC. (b) Contrast of the ECD switched using PEDOT/IL ESC with different PEDOT film thicknesses (polymerization charge density: 120, 360, or 480 mC/cm^2).

self-discharge experiment, we observed an initial 30% drop in the cell voltage during the first 50 min, followed by a slower, more linear decay. For our PEDOT ESCs the $1/2V_{max}$ point, which is commonly used for evaluating ESCs, is 7.0 ± 0.5 h. For comparison, we performed the same measurement on a commercially available 25 mF/3.5 V ESC and noted a self-discharge time of 8 h (V_{max} to $1/2V_{max}$).[40] We chose this particular ESC, as it most closely matched the absolute capacitance attainable by a PEDOT ESC-360/IL (10.5 mF/cm^2, i.e. ∼30 mF). The leakage current is a measure of the current required to maintain a certain voltage, typically V_{max}. Figure 7b shows the leakage current experiment for an ESC-360 charged continuously to 1.0 V for 12 h. The recorded leakage current was 2 μA. The corresponding number for the commercially available ESC we used for comparison was 5 μA. The self-discharge times and leakage currents were approximately the same for ESC-120 and ESC-480.

Demonstration of ESC-Powered Electrochromic Devices. In the literature, reported ESC values are rarely placed in a context that provides understanding of how they meet the demands of real world applications. To demonstrate the efficacy of our devices, PEDOT-ESCs were used as the sole power source to switch an electrochromic device (ECD). ECDs were chosen for this demonstration for three reasons. First, electrochromic devices have low operational power requirements and can be switched from a fully colored to a fully colorless state within a small voltage window. In the case of the ECD used here, full contrast was obtained within a 1.5 V window. Second, EAP ECDs maintain their coloration without the need for a constant power supply, such as a battery. Finally, to realize electrochromic displays that are mechanically flexible, an equally flexible power source will be required for operation.

The ECD was constructed using a ProDOT-based polymer (ECP-Magenta)[31] deposited on the working electrode as the electrochromic material and a colorless dioxypyrrole-based polymer (MCCP)[32] on the counter electrode for charge balance. From the current measured during device switching between 1 V to −0.5 V shown in Supporting Information Figure S4, it was calculated that 1.46 mC/cm^2 (or 2.35 mC) and a power of 0.0106 W are required to fully switch between the colored and colorless states. To power the ECD, a fully charged ESC was then connected to the ECD, as shown in the diagram in Supporting Information Figure S5 and demonstrated in Figure 8. Starting with a fully charged ESC and the ECD in its colored state, as shown in Figure 8a, connecting the working electrodes leads to current flowing from the ESC to the ECD, discharging the ESC and in the process switching the ECD from its colored to its colorless state, as shown in Figure 8b. Upon reverse-bias, current flows from the ECD to the ESC causing the ECD to switch back to the colored state in Figure 8a while partially recharging the ESC.

To demonstrate the effectiveness of the PEDOT-ESC as a power source, we compared the kinetic and spectroscopic properties of the ECD when switched using a PEDOT-ESC with respect to the ECD when switched using a potentiostat. The properties of the ECD switched with a potentiostat serve as a standard for the properties of the ECD switched using a PEDOT-ESC, as more controlled rates of charging/discharging

as well as potentials can be obtained. Photographs and spectra of the device in its fully colored and fully colorless states were found to be identical regardless if switched using a potentiostat (applied bias of −0.5 V for the colored state and 1.0 V for the colorless state) or PEDOT-ESCs. The spectra of the ECD switched with the ESC are shown in Figure 9a. In Figure 9b, the contrast range attainable for an ECD evaluated at λ_{max} was assessed over the course of 10 cycles. In the first cycle, the ECD attained the same contrast window when switched either with a potentiostat or with a PEDOT-ESC, irrespective of the amount of PEDOT in the ESC. Additionally, the time for the ECD to reach maximum contrast was also found to be largely independent of this parameter, as shown in Supporting Information Figure S6. From Table 1, at the maximum rate of discharge, ESC-360 is calculated to deliver a sufficient amount of power in approximately 1 s for full switching of the ECD, which is in good agreement with the observed switching speed in Supporting Information Figure S6. However, the amount of PEDOT in the ESC was found to correlate with the number of full-contrast switches the ECD could achieve from one fully charged PEDOT-ESC, as shown in Figure 9b. A PEDOT-ESC using a polymerization charge of 120 mC/cm^2 provided one full-contrast switch, while ESCs using three and four times the polymerization charge afforded nearly three and four full-contrast switches. The increasing number of full-contrast switches attainable corresponds to the increase in capacitance as the amount of active material in PEDOT-ESCs increases. In all cases, the ECD contrast window decreased over the course of 10 cycles, with devices switched using ESC-480 showing the most gradual decrease until a recharge of the ESC was needed. These initial results demonstrate the ability of our ESCs to repeatedly switch a low-power electrochromic device between its maximum contrast range at charge and discharge rates comparable to contrasts and rates achieved with a potentiostat.

CONCLUSIONS

In summary, a number of steps were taken to maximize the performance of PEDOT ESCs and highlight their promise. First, the electrodeposition conditions of PEDOT films were optimized to obtain systems with the highest capacitance. Devices fabricated from these films were assembled then using various electrolytes, which in turn were found to tune the fill factor of the device CVs, with the IL [EMI][BTI] offering the highest fill factor. Additionally, ILs extended the voltage window of device operation (from 1.0 to 1.6 V), allowing for improved energy and power densities (2.5-fold and 1.6-fold increases, respectively). Further device testing illustrated the relationship between polymer loading, energy density, and power density, showing that while energy density scales with polymer loading, the behavior of power density is more subtle. Device performance was assessed based on figures-of-merit that are critical to evaluating the practical value of EAP ESCs. Our devices were found to be highly stable over hundreds of thousands of cycles, possessing low leakage currents, and slow self-discharge. Finally, its applicability was demonstrated by fully powering a high-contrast and fast-switching electrochromic device for a number of cycles that depended on the polymer loading. These results establish EAP ESCs as competitive devices in the field, capable of being integrated into flexible and low-power organic electronic systems.

ASSOCIATED CONTENT

Supporting Information

Figures S1−S6 as described in the text. This information is available free of charge via the Internet at http://pubs.acs.org.

AUTHOR INFORMATION

Corresponding Author

*E-mail: anna.osterholm@chemistry.gatech.edu.

Author Contributions

The manuscript was written through contributions of all authors. All authors have given approval to the final version of the manuscript.

Notes

The authors declare no competing financial interest.

ACKNOWLEDGMENTS

The authors gratefully acknowledge Mr. James Ponder for the synthesis of [EMI][BTI] and the Office of Naval Research, Capacitor Program (Grant: N00014-12-1-0446) and BASF for financial support of this work.

REFERENCES

(1) Clarke, T. M.; Durrant, J. R. *Chem. Rev.* **2010**, *110*, 6736−6767.
(2) Thompson, B. C.; Fréchet, J. M. J. *Angew. Chem., Int. Ed.* **2008**, *47*, 58−77.
(3) Beaujeuge, P. M.; Reynolds, J. R. *Chem. Rev.* **2010**, *110*, 268−320.
(4) Dyer, A. L.; Reynolds, J. R. In *Handbook of Conducting Polymers*, 3rd ed.; Skotheim, T. A.; Reynolds, J. R., Eds.; CRC Press: Boca Raton, 2007; 20/1.
(5) Rudge, A.; Raistrick, I.; Gottesfeld, S.; Ferraris, J. P. *Electrochim. Acta* **1994**, *39*, 273−287.
(6) Irvin, J. A.; Stenger-Smith, J. D. In *Handbook of Conducting Polymers: Processing and Applications*, 3rd ed.; Skotheim, T. A.; Reynolds, J. R., Eds.; CRC Press: Boca Raton, 2007; 9/1.
(7) Snook, G. A.; Kao, P.; Best, A. S. *J. Power Sources* **2011**, *196*, 1−12.
(8) Winter, M.; Brodd, R. J. *Chem. Rev.* **2004**, *104*, 4245−4270.
(9) Pandolfo, A. G.; Hollenkamp, A. F. *J. Power Sources* **2006**, *157*, 11−27.
(10) Miller, J. R. *Science* **2012**, *335*, 1312−1313.
(11) Simon, P.; Gogotsi, Y. *Nat. Mater.* **2008**, *7*, 845−854.
(12) Rudge, A.; Davey, J.; Raistrick, I.; Gottesfeld, S.; Ferraris, J. P. *J. Power Sources* **1994**, *47*, 89−107.
(13) Cho, S.; Kwon, W. J.; Choi, S.-J.; Kim, P.; Park, S.-A.; Kim, J.; Son, S. J.; Xiao, R.; Kim, S.-H.; Lee, S. B. *Adv. Mater.* **2005**, *17*, 171−175.
(14) Liu, R.; Cho, S. I.; Lee, S. B. *Nanotechnology* **2008**, *19* (215710), 1−8.
(15) Stoller, M. D.; Ruoff, R. S. *Energy Environ. Sci.* **2010**, *3*, 1294−1301.
(16) Brandt, A.; Pohlmann, S.; Varzi, A.; Balducci, A.; Passerini, S. *MRS Bull.* **2013**, *38*, 554−559.
(17) Hapiot, P.; Lagrost, C. *Chem. Rev.* **2008**, *108*, 2238−2264.
(18) Galinski, M.; Lewandowski, A.; Stepniak, I. *Electrochim. Acta* **2006**, *51*, 5567−5580.
(19) Ding, J.; Zhou, D.; Spinks, G.; Wallace, G.; Forsyth, S.; Forsyth, M.; MacFarlane, D. *Chem. Mater.* **2003**, *15*, 2392−2398.
(20) Stenger-Smith, J. D.; Webber, C. K.; Anderson, N.; Chafin, A. P.; Zong, K.; Reynolds, J. R. *J. Electrochem. Soc.* **2002**, *149*, A973−A977.
(21) Stenger-Smith, J. D.; Lai, W. W.; Irvin, D. J.; Yandek, G. R.; Irvin, J. A. *J. Power Sources* **2012**, *220*, 236−242.
(22) Lu, W.; Fadeev, A. G.; Qi, B.; Mattes, B. R. *J. Electrochem. Soc.* **2004**, *151*, H33−H39.
(23) Groenendaal, L.; Zotti, G.; Aubert, P.-H.; Waybright, S. M.; Reynolds, J. R. *Adv. Mater.* **2003**, *15*, 855−879.

(24) Ryu, K. S.; Lee, Y.-G.; Hong, Y.-S.; Park, Y. J.; Wu, X.; Kim, K. M.; Kang, M. G.; Park, N.-G.; Chang, S. H. *Electrochim. Acta* **2004**, *50*, 843−847.
(25) Jonas, F.; Schrader, L. *Synth. Met.* **1991**, *41*−*43*, 831−836.
(26) Liu, D.; Reynolds, J. R. *ACS Appl. Mater. Interfaces* **2010**, *2*, 3586−3593.
(27) Stenger-Smith, J. D.; Guenthner, A.; Cash, J.; Irvin, J. A.; Irvin, D. J. *J. Electrochem. Soc.* **2010**, *157*, A298−A304.
(28) Burrell, A. K.; Del Sesto, R. E.; Baker, S. N.; McCleskey, T. M.; Baker, G. A. *Green Chem.* **2007**, *9*, 449−454.
(29) Lu, W.; Henry, K.; Turchi, C.; Pellegrino, J. *J. Electrochem. Soc.* **2008**, *155*, A361−A367.
(30) Stenger-Smith, J. D.; Irvin, J. A. *Mater. Matters* **2009**, *4* (4), 103.
(31) Reeves, B. D.; Grenier, C. R. G.; Argun, A. A.; Cirpan, A.; McCarley, T. D.; Reynolds, J. R. *Macromolecules* **2004**, *37*, 7559−7569.
(32) Knott, E. P.; Craig, M. R.; Liu, D. Y.; Babiarz, J. E.; Dyer, A. L.; Reynolds, J. R. *J. Mater. Chem.* **2012**, *22*, 4953−4962.
(33) Kim, Y.; Kim, H.; Graham, S.; Dyer, A.; Reynolds, J. R. *Sol. Energy Mater. Sol. Cells* **2012**, *100*, 120−125.
(34) Deepa, M.; Sharma, N.; Agnihotry, S. A.; Singh, S.; Lal, T.; Chandra, R. *Solid State Ionics* **2002**, *152*−*153*, 253−258.
(35) Pandey, G. P.; Rastogi, A. C. *J. Electrochem. Soc.* **2012**, *159*, A1664−A1671.
(36) Irvin, J. A.; Carberry, J. R. *J. Polym. Sci., Part B: Polym. Phys.* **2013**, *51*, 337−342.
(37) Randriamahazaka, H.; Plesse, C.; Teyssié, P. D.; Chevrot, C. *Electrochem. Commun.* **2004**, *6*, 299−305.
(38) Lu, W.; Fadeev, A. G.; Qi, B.; Smela, E.; Mattes, B. R.; Ding, J.; Spinks, G. M.; Mazurkiewicz, J.; Zhou, D.; Wallace, G. G.; MacFarlane, D. R.; Forsyth, S. A.; Forsyth, M. *Science* **2002**, *297*, 983−987.
(39) Pringle, J. M.; Forsyth, M.; MacFarlane, D. M.; Wagner, K.; Hall, S. B.; Officer, D. L. *Polymer* **2004**, *45*, 1447−1453.
(40) Flat leads Cellergy Supercapacitor, 25 mF/3.5 V